

Original Research Article

Azaindole inhibits liver cancer cell proliferation *in vitro* and *in vivo* by targeting the expression of kinesin family member C1

Zhen You¹, Bei Li¹, Jun Gao², Jiong Lu¹, Ruihua Xu^{1*}

¹Department of Biliary Surgery, Westchina Hospital of Sichuan University, ²Department of Toxicological Inspection, Sichuan Centre for Disease Prevention and Control, Chengdu, Sichuan 610041, China

*For correspondence: **Email:** ruihuaxuo41@gmail.com; **Tel/Fax:** 0086-028-85422114

Sent for review: 15 September 2020

Revised accepted: 23 January 2021

Abstract

Purpose: To investigate the effect of azaindole on proliferation of liver cancer cells, as well as the underlying mechanism.

Methods: Colony forming and 3-(4,5-dimethylthiazole-2-yl)-2,5-biphenyl tetrazolium bromide (MTT) assays were used to determine the effect of azaindole on cell proliferation. A tumor model was established through subcutaneous administration of HEPG2 cells to rats. Thereafter, *in vivo* tumor development was measured using Vernier caliper.

Results: The proliferation potential of HEPG2 and SNU-398 cells was markedly and dose-dependently suppressed by treatment with azaindole at doses of 2, 4, 8, 16 and 20 μ M ($p < 0.05$). The expression levels of Ki67 and PCNA levels were significantly down-regulated in HEPG2 and SNU-398 cells on treatment with 20 μ M azaindole. Moreover, azaindole significantly suppressed mRNA and protein expressions of KIFC1 in HEPG2 and SNU-398 cells ($p < 0.05$). Tumor volume in azaindole-treated rats on day 21 was greatly reduced, while KIFC1 expression in azaindole-treated rat tumor tissue was significantly down-regulated, when compared to the model group ($p < 0.05$).

Conclusion: Azaindole targets proliferation of liver cancer cells *in vitro* and inhibits tumor growth *in vivo* through a mechanism involving down-regulation of KIFC1 expression. Thus, azaindole is a potential therapeutic candidate for liver cancer.

Keywords: Liver cancer, Azaindole, Malignant tumor, Kinesin, Antartic sponge

This is an Open Access article that uses a fund-ing model which does not charge readers or their institutions for access and distributed under the terms of the Creative Commons Attribution License (<http://creativecommons.org/licenses/by/4.0>) and the Budapest Open Access Initiative (<http://www.budapestopenaccessinitiative.org/read>), which permit unrestricted use, distribution, and reproduction in any medium, provided the original work is properly credited.

Tropical Journal of Pharmaceutical Research is indexed by Science Citation Index (SciSearch), Scopus, International Pharmaceutical Abstract, Chemical Abstracts, Embase, Index Copernicus, EBSCO, African Index Medicus, JournalSeek, Journal Citation Reports/Science Edition, Directory of Open Access Journals (DOAJ), African Journal Online, Bioline International, Open-J-Gate and Pharmacy Abstracts

INTRODUCTION

Liver cancer is a malignant tumor which is ranked the third highest cause of mortality throughout the world [1]. In China, liver cancer is most commonly diagnosed in cirrhotic patients, and such cases usually result in high mortality [2]. The rise in viral infections,

especially hepatitis c, has led to a significant increase in incidence of liver cancer in USA and many developing countries [3]. Hepatic resection is usually followed by recurrence and metastasis, resulting in very low long-term survival of liver cancer patients [4]. Identification of targets and associated pathways of liver cancer is very useful for development of

efficient treatments for the disease. However, the involvement of multiple genes and several proteins in the etiology of liver cancer complicates the pathogenesis of this disease [5].

Kinesin family member C1 (KIFC1; also represented as HSET) is an important member of the kinesin superfamily [6]. The movement of KIFC1 in microtubules towards minus-end is associated with the ciliogenesis and development of spindle bodies [7]. Moreover, KIFC1 induces proper positioning of the Golgi apparatus so as to facilitate transport processes [8]. It is known that KIFC1 plays an important role in tumorigenesis. Excessive KIFC1 expression has been reported in multiple tumor types, including renal and lung cancers [9]. In cancer patients, the rate of cell proliferation and chances of survival are largely influenced by KIFC1 expression [9]. Moreover, in patients with triple-negative breast cancer, nuclear KIFC1 is an indicator of poor prognosis [10]. Previous studies have shown that KIFC1 is associated with the etiology and metastasis of tumors [11]. Moreover, it has been reported that KIFC1 induces docetaxel resistance and poor prognosis in prostate cancer patients [12].

The Antarctic sponge, *Kirkpatrickia variolosa* contains several phytoconstituents, including variolins which are 7-azaindoles. These 7-azaindole-containing alkaloid skeletons were later found to be active against several diseases/disorders [13,14]. The 7-azaindoles act as agrochemicals, and as protoplasm vacuolation inducers, besides having anti-leukemia properties [13,14]. In the current study, the effect of azaindole on liver cancer cell proliferation and tumor growth was investigated.

EXPERIMENTAL

Cell culture

The HEPG2 and SNU-398 cell lines were provided by the American Type Culture Collection (ATCC). The cells were maintained in RPMI-1640 medium (Thermo Fisher Scientific, Inc.) containing 10 % FBS, and were cultured at 37 °C in an incubator with humidified 5 % CO₂ atmosphere.

MTT assay

The HEPG2 and SNU-398 cells were seeded in 96-well plates, each at density of 1 x 10⁵ cells/well. Then, the cells were incubated for 48 h with azaindole at doses of 2, 4, 8, 16 and 20 µM. Thereafter,

3-(4,5-dimethylthiazole-2-yl)-2,5-biphenyl tetrazolium bromide (MTT) was added to each plate, and cell incubation was continued for additional 4 h. This was followed by replacement of the medium in each well with DMSO (150 µL) so as to solubilize the resultant formazan crystals. The optical density of the formazan solution in each well was read at 570 nm using a microplate reader, and the values obtained were used for determination of cell proliferation.

Colony formation assay

In 6-well culture plates, HEPG2 and SNU-398 cells were seeded, each at a density of 1 x 10⁵ cells/well, and incubated with 20 µM azaindole for 14 days. Thereafter, the cells were fixed with 4 % paraformaldehyde and stained for 20 min with crystal violet to determine colony-forming potential. Images of the colonies were captured. Moreover, absorbance measurements were made at 570 nm using microplate reader.

Western blot analysis

Following treatment with azaindole (20 µM) for 48 h, the cells were lysed using CellLytic™ M reagent (Sigma-Aldrich). The lysate was centrifuged at 4 °C for 15 min at 12000 g, and the protein content of the supernatant was determined using bicinchoninic acid (BCA) assay kit. The samples (30 µg/lane) were subjected to 8-10 % SDS-polyacrylamide gel electrophoresis, followed by transfer to PVDF membranes which were subsequently blocked with goat serum for 1 h. Then, the membranes were incubated overnight at 4 °C with anti-KIFC1, anti-PCNA, anti-Ki67 and β-actin primary antibodies. Thereafter, the membranes were washed with PBS, followed by 1 h incubation with goat anti-rabbit secondary antibody at room temperature. Coomassie brilliant blue G-250 was used for band visualization, while analysis of gray scale values was done with Odyssey v3.0 software.

Quantitative reverse transcription-polymerase chain reaction (qRT-PCR)

Total RNA was extracted from 20 µM azaindole-treated cells using TRIzol® reagent (Invitrogen). Reverse transcription of the total RNA was carried out using M-MLV transcriptase consisting of template RNA (10 µl) and primers, prime Script (1 µL), H₂O (20 µL) and 5x Prime Script buffer (4 µl). The reaction mixture was incubated for 1 h at 42 °C, and then for 20 min at 70 °C. The SYBR Green PCR Master Mix (Thermo Fisher Scientific, Inc.) was used for qRT-PCR under the following thermocycling conditions:

initial denaturation for 6 min at 94 °C, 38 cycles for 25 sec at 95 °C, 28 sec at 64 °C, 40 sec at 72 °C, and 8 min at 72 °C. The products of PCR were subjected to electrophoresis using agarose gel, followed by scanning with gel imaging system. The relative mRNA expression level was normalized to that of β -actin using $2^{-\Delta\Delta Ct}$ [9]. The sequences of the primers used were:

KIFC1: sense 5'-TGA GCA ACA AGG AGT CCC AC-3'; antisense, 5'-TCA CTT CCT GTT GGC CTG AG-3';

β -actin sense, 5'-CAG CTC ACC ATG GAT GAT GAT ATC-3'; anti-sense, 5'-AAG CCG GCC TTG CAC AT-3'.

Establishment of a rat tumor model

In the *in vivo* studies, a total of 50 Sprague-Dawley rats (8-week old, weighing 295- 320 g) were purchased from the Harbin Institute of Veterinary Research, China. The animals were housed in an environment with a mean temperature of 23 ± 2 °C and relative humidity of 53 ± 2 %, and were provided free access to laboratory diet and water. The experiment was carried out under 12- h light/12-h dark photoperiod. Study approval (approval no. ASU/02/17/008) was obtained from the Animal Care Committee of the Weifang Medical University, China. All animal experimental protocols were performed in accordance with the guidelines issued by the National Institute of Health, US. The tumor model was established by implanting HEPG2 cells (2×10^5) subcutaneously into the right flank of the rats. Then, the rats were randomly assigned to five groups: sham, model and three azaindole treatment groups given the drug at doses of 2, 4 and 5 mg/kg. Azaindole was injected daily into rats in the three treatment groups for 20 days via the intraperitoneal route. Following HEPG2 cell implantation, tumor volume was measured every 4 days for 20 days using Vernier caliper. Thereafter, the rats were sacrificed using cervical dislocation under sodium sorbitol anesthesia.

Analysis of KIFC1 expression

Tumor specimens were fixed in 10 % formaldehyde, and 3- μ m tissue sections were embedded in paraffin. De-paraffinization and subsequent rehydration in xylene and gradient ethyl alcohol were followed by treatment with citrate buffer, pH 6.0 at 140 °C (for antigen retrieval). Then, the tissues were treated with 3 % H_2O_2 for 15 min to inactivate endogenous peroxidases. Thereafter, the tissues were blocked by treatment with 5 % BSA at 4°C for

30 min, followed by incubation for 2 h with anti-KIFC1 antibodies at 37 °C. Then, the tissues were incubated with goat anti-rabbit immunoglobulin G secondary antibody at 37 °C for 2 h, with 3,3'-diaminobenzidine as chromogen substrate. Subsequently, the tissues were examined under a light microscope at x200 magnification.

Statistical analysis

Data analysis was performed using SPSS version 22.0 software (IBM Corp.). All data are presented as mean \pm standard deviation (SD). Differences were determined using one-way ANOVA and Student-Newman-Keuls test. Differences were considered statistically significant at $p < 0.05$.

RESULTS

Azaindole inhibited proliferation of HEPG2 and SNU-398 cells

Azaindole treatment for 48 h significantly and dose-dependently inhibited the proliferations of HEPG2 and SNU-398 cells (Figure 1 A). At doses of 2, 4, 8, 16 and 20 μ M, azaindole decreased the proliferative potential of HEPG2 cells to 90, 74, 59, 42 and 28 %, respectively. In SNU-398 cells, azaindole exposure reduced the proliferation to 88, 71, 54, 40 and 25 %, at 2, 4, 8, 16 and 20 μ M, respectively. Colony forming assay also confirmed the azaindole-induced reduction in the proliferations of HEPG2 and SNU-398 cells (Figure 1 B). Moreover, at a dose of 20 μ M, azaindole markedly inhibited the growth of colonies formed by HEPG2 and SNU-398 cells, when compared to the untreated cells ($p < 0.05$).

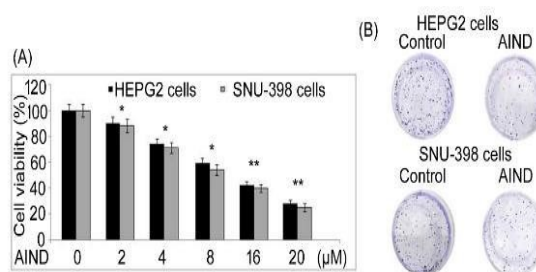


Figure 1: Effect of azaindole on proliferative potential of HEPG2 and SNU-398 cells. (A) Viability of HEPG2 and SNU398 cells at 48 h of azaindole treatment, as measured using MTT assay. (B) Colony formation after treatment of HEPG2 and SNU-398 cells with azaindole at indicated doses for 48 h. * $P < 0.05$, ** $p < 0.02$, vs. untreated cells

Azaindole suppressed levels of proliferation biomarkers

The expression levels of Ki67 in HEPG2 and SNU-398 cells on treatment with 20 μ M azaindole were markedly lower than the corresponding expression levels in untreated control cells (Figure 2). Azaindole treatment also caused marked reductions in PCNA expression levels in HEPG2 and SNU-398 cells at 48 h. Thus, in HEPG2 and SNU-398 cells, azaindole treatment significantly targeted the proliferation biomarkers.

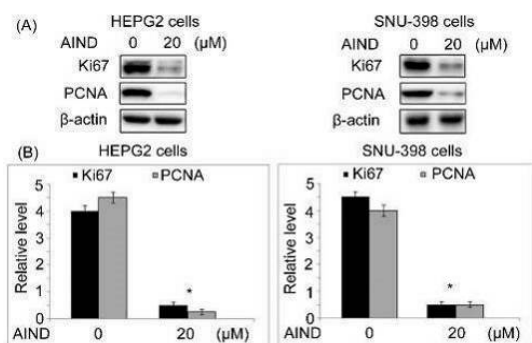


Figure 2: Effect of azaindole on proliferation biomarker levels. (A) Expressions Ki67 and PCNA at 48 h following treatment of HEPG2 and SNU-398 cells with 20 μ M azaindole. (B) Quantified expression levels of Ki67 and PCNA at 48 h. * $P < 0.02$, vs. untreated cells

Azaindole targeted KIFC1 expression

In HEPG2 and SNU-398 cells, treatment with 20 μ M azaindole was followed by analysis of protein expression levels of KIFC1 (Figure 3). The KIFC1 protein levels were significantly reduced in HEPG2 and SNU-398 cells on treatment with azaindole. Moreover, azaindole treatment for 48 h significantly ($p < 0.05$) suppressed the mRNA expression levels of KIFC1 in HEPG2 and SNU-398 cells.

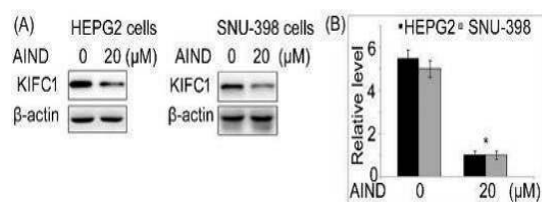


Figure 3: Effect of azaindole on KIFC1 expressions in HEPG2 and SNU-398 cells. (A) KIFC1 protein expression levels at 48 h, as assayed using Western blotting. (B) mRNA expression levels of KIFC1 after treatment of HEPG2 and SNU-398 cells with 20 μ M azaindole, as assayed using RT-PCR. * $P < 0.05$ vs. untreated cells

Azaindole targeted tumor proliferation *in vivo*

Tumor volume in azaindole-treated rats on day 21 was much smaller than tumor volume in the model group (Figure 4). Azaindole-induced decreases in tumor volume on day 21 were significant at doses of 2, 4 and 5 mg/kg, when compared to model rat group.

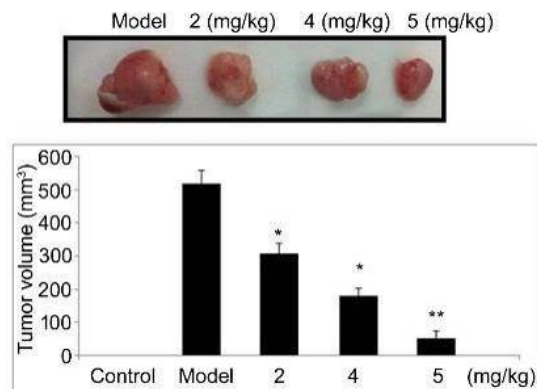


Figure 4: Effect of azaindole on tumor volume in rats. Treatment with azaindole at doses of 2, 4 and 5 mg/kg was followed by tumor excision and measurement of tumor volume on day 21. * $P < 0.05$, ** $p < 0.02$, vs. model rats

Azaindole targeted KIFC1 *in vivo*

Figure 5 shows KIFC1 expression levels in tumor tissues of rats treated with azaindole (5 mg/kg), as assayed using Western blotting (Figure 5). The KIFC1 expression in azaindole-treated rat tumor tissues was significantly lower than that in model rat group ($p < 0.05$). Thus, azaindole treatment also targeted KIFC1 expression *in vivo* in rat model of liver cancer.

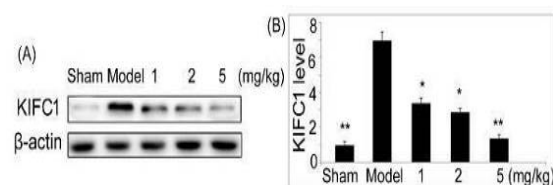


Figure 5: Effect of azaindole on KIFC1 expression *in vivo*. Treatment with azaindole (5 mg/kg) was followed by tumor excision on day 21 for determination of KIFC1 expression using Western blotting. ** $P < 0.02$ vs. model rats

DISCUSSION

Rapid metastasis and tumor heterogeneity are responsible for high mortality in liver cancer patients, and they pose major obstacles to radiotherapy and chemotherapy [15]. Target-

oriented therapies have been confirmed to be more effective for liver cancer treatment than traditional methods [16]. In the present study, azaindole significantly and dose-dependently inhibited the proliferations of HEPG2 and SNU-398 cells. The azaindole-induced toxicity on HEPG2 and SNU-398 cells was confirmed using colony forming assay which demonstrated that the growth of colonies formed by HEPG2 and SNU-398 cells was markedly suppressed by azaindole, relative to untreated cells. Moreover, in HEPG2 and SNU-398 cells, azaindole effectively targeted the expressions of proliferation biomarkers.

The expression levels of Ki67 and PCNA in azaindole-treated HEPG2 and SNU-398 cells were markedly lower than the corresponding expression levels in untreated control cells. Identification of novel drug targets such as monocarboxylate transporter-4 for inhibition of tumor growth and metastasis is considered an effective therapeutic strategy for cancer [17]. Studies have shown that KIFC1 expression is associated with tumor growth in many types of cancers, suggesting that it may be a useful target for cancer treatment [15,17]. It has been reported that KIFC1 enhances spindle formation via interaction with microtubules, regulates amplification of centrosome, and promotes development of monopolar spindles in tumor cells [18,19]. Poor prognosis in various cancers has been linked to the expression of KIFC1 which enhances proliferation of tumor cells [9,10].

In cancer cells, transport of vesicles has a crucial role which is regulated by KIFC1 expression [20]. A previous study indicated that KIFC1 may act as a link between the Golgi apparatus and microtubules by regulating the positioning and structure of the Golgi apparatus [8]. Tumor development is controlled by several members of kinesin family such as KIF3B and KIF14 [21]. In breast carcinoma cells, elevated expression of KIFC1 has been associated with high degree of proliferation and increased cell migration [22]. In the present study, azaindole treatment suppressed the mRNA and protein expressions of KIFC1 in HEPG2 and SNU-398 cells, thereby inhibiting cell growth. The tumor volume in azaindole-treated rats was much smaller than that in untreated tumor model rats. The azaindole-induced decrease in tumor volume was significant on day 21, when compared to model rat group, and KIFC1 expression level in azaindole-treated rat tumor tissues was significantly lower than that in model rat group.

CONCLUSION

Azaindole targets the proliferation of liver cancer cells *in vitro*, and inhibits growth of tumor *in vivo*. Treatment of liver cancer cells with azaindole markedly down-regulated KIFC1 expression, when compared to untreated control cells. Thus, azaindole may be used as a potential candidate for treatment of liver cancer

DECLARATIONS

Conflict of interest

No conflict of interest is associated with this work.

Contribution of authors

We declare that this work was done by the authors named in this article, and all liabilities pertaining to claims relating to the content of this article will be borne by the authors. Ruihua Xu designed the study and wrote the manuscript. Zhen You, Lei Li, Jun Gao, Jiong Lu performed the experimental work. Zhen You, Lei Li carried out the literature survey and compiled the data. Jun Gao, Jiong Lu performed literature survey, and compiled and analysed the data. The manuscript was thoroughly read by all the authors before communication for consideration of its publication.

Open Access

This is an Open Access article that uses a funding model which does not charge readers or their institutions for access and distributed under the terms of the Creative Commons Attribution License (<http://creativecommons.org/licenses/by/4.0>) and the Budapest Open Access Initiative (<http://www.budapestopenaccessinitiative.org/read>), which permit unrestricted use, distribution, and reproduction in any medium, provided the original work is properly credited.

REFERENCES

- Hernandez-Gea V, Turon F, Berzigotti A, Villanueva A. Management of small hepatocellular carcinoma in cirrhosis: Focus on portal hypertension. *World J Gastroenterol* 2013; 19: 1193-1199.
- Ziogas IA, Tsoulfas G. Advances and challenges in laparoscopic surgery in the management of hepatocellular carcinoma. *World J Gastrointest Surg* 2017; 9: 233-245.
- Kim D, Li AA, Perumpail BJ, Gadiparthi C, Kim W, Cholankeril G, Glenn JS, Harrison SA, Younossi ZM,

- Ahmed A. Changing trends in etiology-based and ethnicity-based annual mortality rates of cirrhosis and hepatocellular carcinoma in the United States. *Hepatology* 2019; 69: 1064-1074.
4. Yang LY, Fang F, Ou DP, Wu W, Zeng ZJ, Wu F. Solitary large hepatocellular carcinoma: A specific subtype of hepatocellular carcinoma with good outcome after hepatic resection. *Ann Surg* 2009; 249: 118-123.
 5. Karavias D, Maroulis I, Papadaki H, Gogos C, Kakkos S, Karavias D, Bravou V. Overexpression of CDT1 is a predictor of poor survival in patients with hepatocellular carcinoma. *J Gastrointest Surg* 2016; 20: 568-579.
 6. Ma DD, Pan MY, Hou CC, Tan FQ, Yang WX. KIFC1 and myosin Va: Two motors for acrosomal biogenesis and nuclear shaping during spermiogenesis of *Portunus trituberculatus*. *Cell Tissue Res* 2017; 369: 625-640.
 7. Lee SH, Joo K, Jung EJ, Hong H, Seo J, Kim J. Export of membrane proteins from the Golgi complex to the primary cilium requires the kinesin motor, KIFC1. *FASEB J* 2018; 32: 957-968.
 8. She ZY, Pan MY, Tan FQ, Yang WX. Minus end-directed kinesin-14 KIFC1 regulates the positioning and architecture of the Golgi apparatus. *Oncotarget* 2017; 8: 36469-36483.
 9. Hou CC, Yang WX. Acroframosome-dependent KIFC1 facilitates acrosome formation during spermatogenesis in the caridean shrimp *Exopalaemon modestus*. *PLoS One* 2013; 8: e76065.
 10. Li G, Chong T, Yang J, Li H, Chen H. Kinesin motor protein KIFC1 is a target protein of miR-338-3p and associated with poor prognosis and progression of renal cell carcinoma. *Oncol Res* 2018; 27: 125-137.
 11. Li Y, Lu W, Chen D, Boohaker RJ, Zhai L, Padmalayam I, Wennerberg K, Xu B, Zhang W. KIFC1 is a novel potential therapeutic target for breast cancer. *Cancer Biol Ther* 2015; 16: 1316-1322.
 12. Sekino Y, Oue N, Shigematsu Y, Ishikawa A, Sakamoto N, Sentani K, Teishima J, Matsubara A, Yasui W. KIFC1 induces resistance to docetaxel and is associated with survival of patients with prostate cancer. *Urol Oncol* 2017; 35: 31.e13-31.e20.
 13. Widholm JM. Tryptophan biosynthesis in *Nicotiana tabacum* and *Daucus carota* cell cultures: Site of action of inhibitory tryptophan analogs. *Biochem. Biophys. Acta* 1972; 261: 44-51.
 14. Minakata S, Hamada T, Komatsu M, Tsuboi H, Kikuta H, Osshiro Y. Synthesis and biological activity of 1H-pyrrolo[2,3-b]pyridine derivatives: correlation between inhibitory activity against the fungus causing rice blast and ionization potential. *J Agric Food Chem* 1997; 45: 2345-2348.
 15. Seino S, Tsuchiya A, Watanabe Y, Kawata Y, Kojima Y, Ikarashi S, Yanai H, Nakamura K, Kumaki D, Hirano M, et al. Clinical outcome of hepatocellular carcinoma can be predicted by the expression of hepatic progenitor cell markers and serum tumour markers. *Oncotarget* 2018; 9: 21844-21860.
 16. DeLeon TT, Ahn DH, Bogenberger JM, Anastasiadis PZ, Arora M, Ramanathan RK, Aqel BA, Vasmatzis G, Truty MJ, Oklu R, et al. Novel targeted therapy strategies for biliary tract cancers and hepatocellular carcinoma. *Future Oncol* 2018; 14: 553-566.
 17. Gao HJ, Zhao MC, Zhang YJ, Zhou DS, Xu L, Li GB, Chen MS, Liu J. Monocarboxylate transporter 4 predicts poor prognosis in hepatocellular carcinoma and is associated with cell proliferation and migration. *J Cancer Res Clin Oncol* 2015; 141: 1151-1162.
 18. Xiao YX, Shen HQ, She ZY, Sheng L, Chen QQ, Chu YL, Tan FQ, Yang WX. C-terminal kinesin motor KIFC1 participates in facilitating proper cell division of human seminoma. *Oncotarget* 2017; 8: 61373-61384.
 19. Mittal K, Choi DH, Klimov S, Pawar S, Kaur R, Mitra AK, Gupta MV, Sams R, Cantuarua G, Rida PCG, Aneja R. A centrosome clustering protein, KIFC1, predicts aggressive disease course in serous ovarian adenocarcinomas. *J Ovarian Res* 2016; 9: 17.
 20. Marsman M, Jordens I, Kuijl C, Janssen L, Neeffes J. Dynein-mediated vesicle transport controls intracellular *Salmonella* replication. *Mol Biol Cell* 2004; 15: 2954-2964.
 21. Huang X, Liu F, Zhu C, Cai J, Wang H, Wang X, He S, Liu C, Yao L, Ding Z, et al. Suppression of KIF3B expression inhibits human hepatocellular carcinoma proliferation. *Dig Dis Sci* 2014; 59: 795-806.
 22. Wang J, Ma S, Ma R, Qu X, Liu W, Lv C, Zhao S, Gong Y. KIF2A silencing inhibits the proliferation and migration of breast cancer cells and correlates with unfavorable prognosis in breast cancer. *BMC Cancer* 2014; 14: 461.